Project: **620**

Project title: **Vertical Propagation of Gravity Waves into the Middle Atmosphere**

Project lead: **Andreas Dörnbrack**

Report period: **2017-01-01 to 2017-12-31**

In the reporting period, the computer time has mainly used to support the finalization of the PhD thesis of Sonja Gisinger and to conduct simulations with a new, fully compressible version of EULAG.

Numerical Simulations with the deep, compressible model aim at two scientific problems:

(1) explore the role of small isolated island in the Southern Ocean on the momentum deposition in the middle atmosphere. As shown by various authors, in most general circulation models the missing gravity wave drag in the mesosphere leads to the so-called "cold-pole" problem, i.e. too strong jets in the Southern Hemisphere isolate the Antarctic stratosphere and generate too low temperatures.

(2) understanding the physics of trapped, non-hydrostatic gravity waves in the middle atmosphere and how are they represented in ground-based and airborne lidar measurements.

To explore the first task, we conducted numerical simulations of one observed case. During DEEPWAVE, airborne measurements have shown the appearance of dispersive mountain waves in about 87 km altitude; see Figure 1.
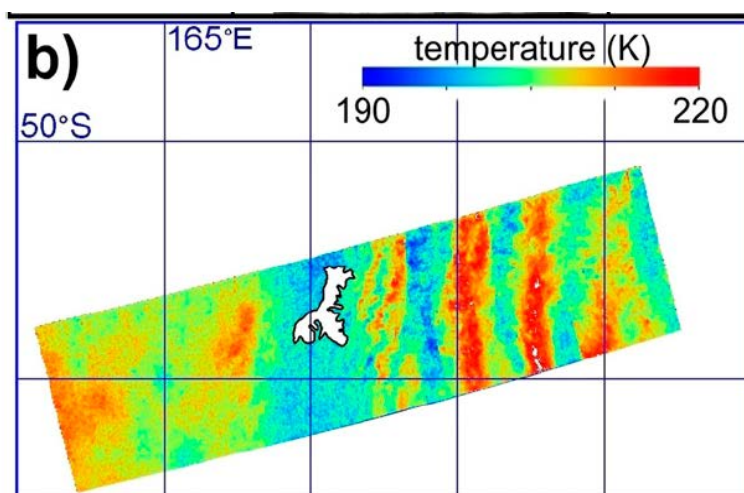


**Figure 1:** Figure 5 from Eckermann et al. (2017) showing the rotational temperature retrieved from the OH airglow brightness at 87 km altitude over and in the lee of the Auckland Islands.
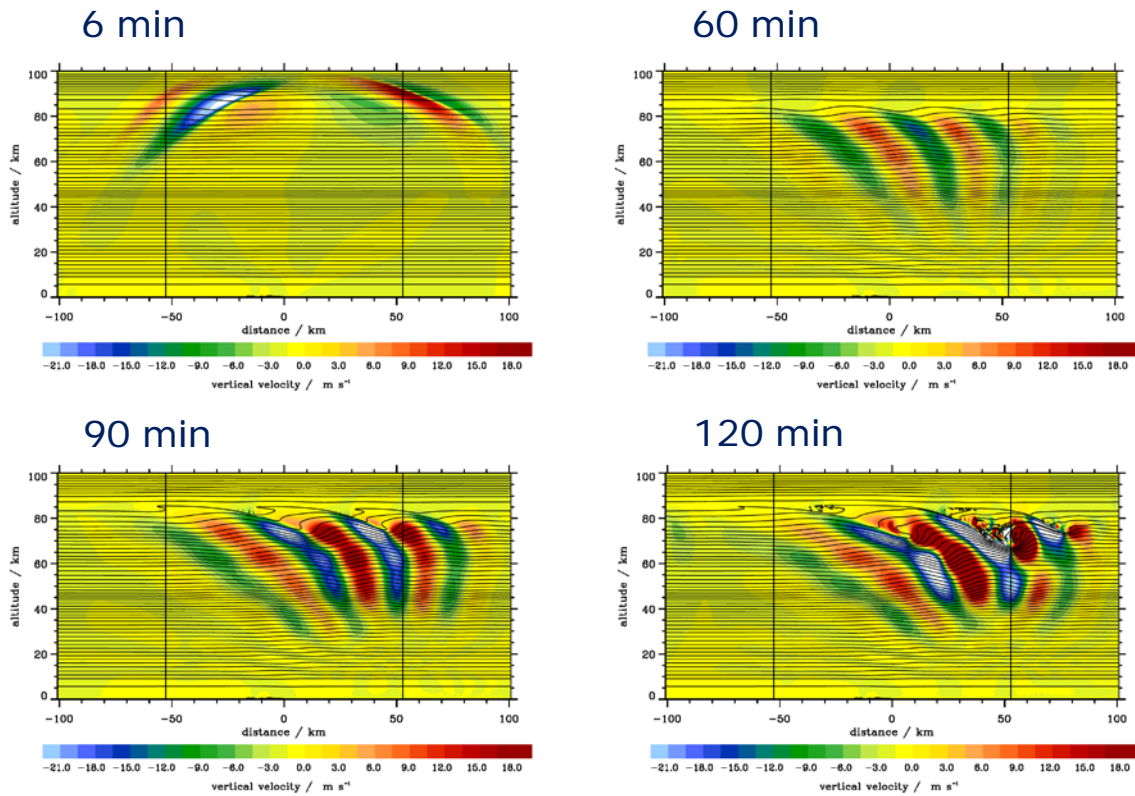
**Figure 2:** Temporal evolution of the vertical wind field from the surface to 100 km altitude above Auckland Islands (located at a horizontal distance between -20 km and 0) for four selected times.

EULAG simulations reveal a quantitatively good agreement of simulated horizontal wavelength with observed wavelength (Fig. 2, t = 90 min). Until wave breaking occurs, the dynamics is essentially linear. Wave breaking happens in gigantic rolls which sit like rotors on the underlying waves, we call these structures mesospheric rotors. The steep, deeply penetrating non-hydrostatic gravity waves (Fig. 2, t = 60 min) act like elevated, quasi-stationary mountains producing „downslope wind storms". They generate broad warm anomalies and narrow cold anomalies like fronts which are also found in the airborne observations. We found a strong dependency of upper air dynamics (z > 60 km) on initial and background profiles. The vertical cross section at t = 6 min shows the resolved sound waves which reach the top of the model domain with the speed of sound.

For the second task, we extended canonical cases of linear mountain wave propagation into the middle atmosphere (Fig. 3 from Dörnbrack et al., 2017). This paper asks the simple question: How can we interpret vertical time series of middle atmosphere gravity wave measurements by ground-based temperature lidars? Linear wave theory is used to show that the association of identified phase lines with quasi-monochromatic waves should be considered with great care. The ambient mean wind has a substantial effect on the inclination of the detected phase lines. The lack of knowledge about the wind might lead to a misinterpretation of the vertical propagation direction of the observed gravity waves. In particular, numerical simulations of three archetypal atmospheric mountain wave regimes show a sensitivity of virtual

lidar observations on the position relative to the mountain and on the scale of the mountain.
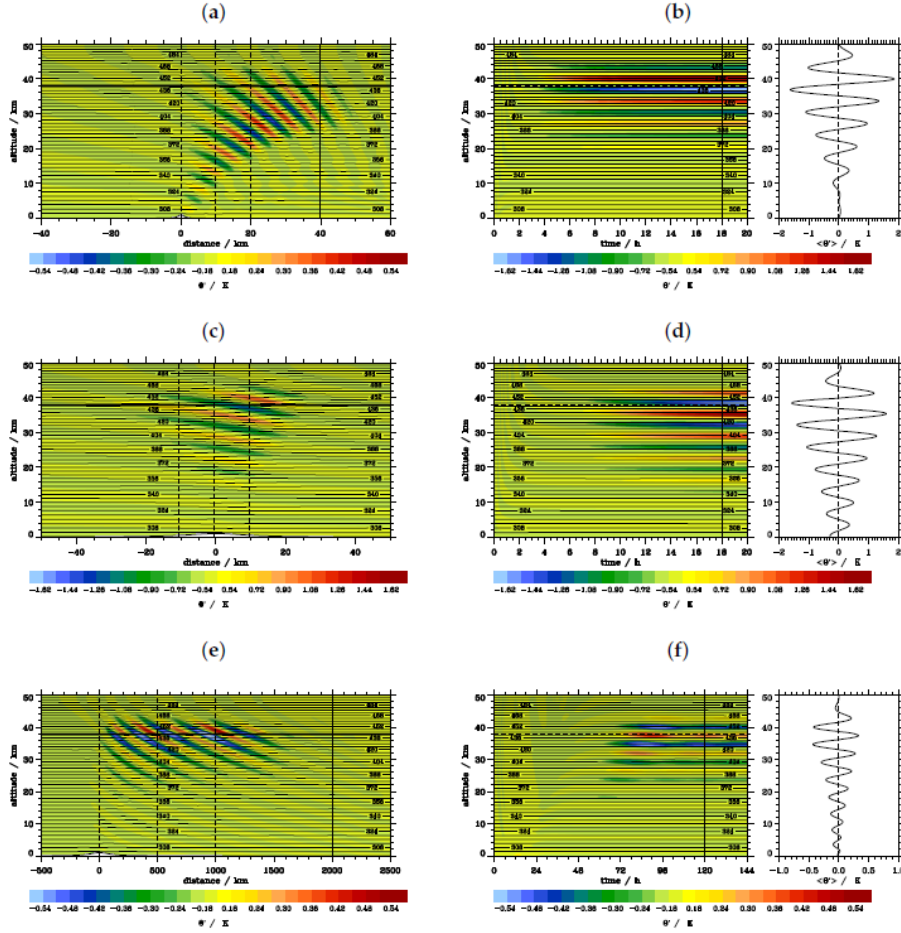


**Figure 3:** Spatial snapshots left (a,c,e) and vertical times series right (b,d,f) of the potential temperature perturbations Θ' for the three different canonical wave regimes. (a,b) non-hydrostatic wave regime; (c,d) hydrostatic nonrotating wave regime; (e,f) hydrostatic rotating wave regime. The right panels in (b,d,f) depict time-averaged Θ'-profiles computed over the period from the time indicated by the vertical line until the end time of the respective panels. The spatial snapshots are taken at t=125 min (a), t=10 h (c) and t=5 d (e). The vertical time series are recorded at x =10 km (b), x 0 0 (d) and x = 500 km (f), as indicated by the vertical dashed lines in (a,c,e). The amplitude of the surface topography is exaggerated by a factor of 10 in (a,c,e).

Fine-scale structures in the troposphere such as sharp temperature inversions can have significant influence on gravity wave and near-surface wind structure (see Vosper (2004) and references therein). An inversion in the troposphere (e.g. at the top of the boundary layer) can be a waveguide for trapped waves which propagate downwind of the mountain. We have investigated if this finding for an inversion in the troposphere can be easily transferred on the tropopause inversion layer. That is based on linear theory and in accordance with the numerical simulations, the Froude number

$$F_i = \frac{U}{\sqrt{g z_i \Delta\theta/\theta}}$$

required for trapping to occur is

$$F_i^2 \le \tanh(Z)/Z,$$

3

where $Z = N z_i/U$, U is the horizontal wind speed, g is gravitational acceleration, $\Delta\theta$ is the strength of the inversion, $\theta$ is potential temperature and $z_i$ is the altitude of the inversion (Vosper, 2004).

The results of the numerical simulations confirm that the concept of trapped waves on an inversion in the troposphere (Fig. 4a) can be applied also to the inversion at the tropopause (Fig. 1b). Thereby, for vertically constant wind speed the strength of the inversion $\Delta\theta$ must be twice as large due to the larger stability of the stratosphere, i.e. $N = 0.02$ s$^{-1}$, for trapping on the inversion to occur and even larger for higher wind speed. Moreover, it was found that reflected waves exist downstream of the mountain in the troposphere although the classical conditions for trapped waves in the troposphere, i.e. a decreasing Scorer parameter with altitude, are not fulfilled. The amplitudes of these reflected waves are found to be larger, if an inversion is present at the tropopause (Fig. 4b) than if there is just the jump from tropospheric to stratospheric stability (Fig. 4c). Horizontal wavelengths of propagating, trapped (on the inversion) and reflected waves increase with increasing wind speed (not shown). The horizontal wavelength of the waves trapped on the inversion decreases with increasing stability above the inversion (Fig. 4a, b).
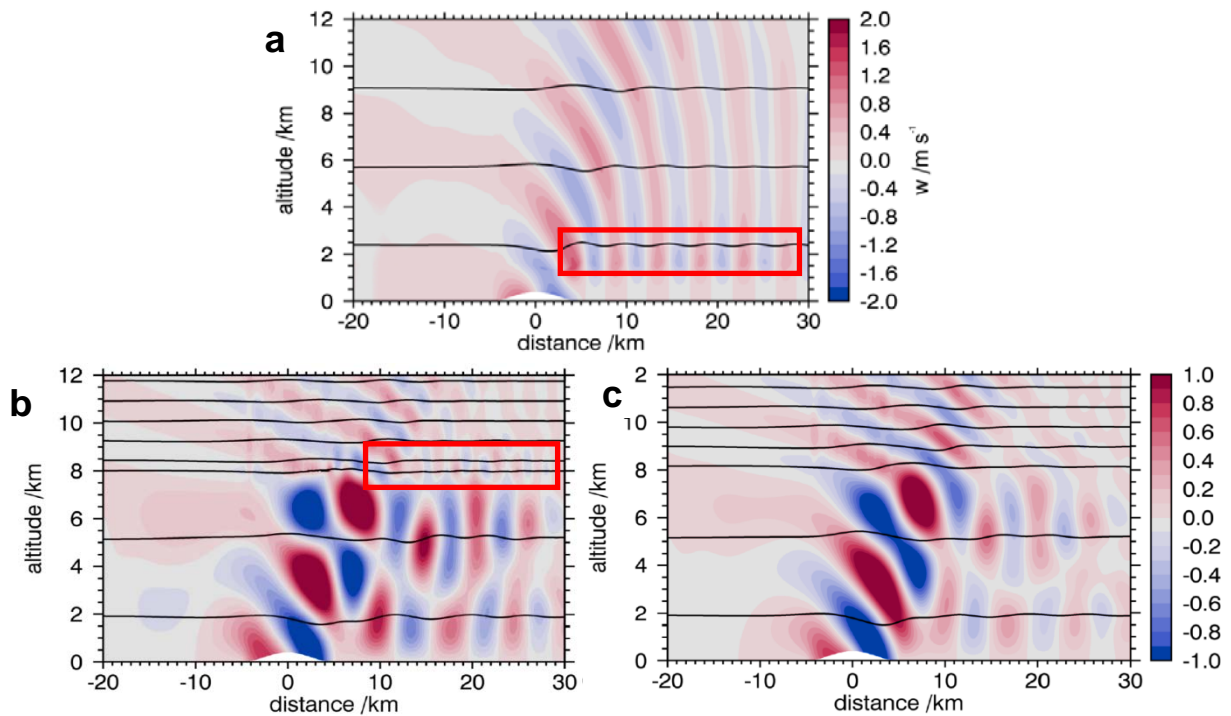


**Figure 4:** Vertical velocity (color) and potential temperature (black lines) of (a) trapped waves on an inversion in the troposphere, (b) trapped waves on a tropopause inversion and reflected waves in the troposphere and (c) no tropopause inversion and only reflected waves in the troposphere.

References:

Dörnbrack, A., S. Gisinger, and B. Kaifler, 2017: On the Interpretation of Gravity Wave Measurements by Ground-Based Lidars. *Atmosphere*, **8**, 1–22. DOI: 10.3390/atmos8030049 ISSN 2073-443.

Gisinger, S., 2017: *Gravity waves in the lower atmosphere in mountainous regions and the role of the tropopause*. Dissertation, submitted to LMU Munich.

Eckermann, S. et al., 2016: Dynamics of Orographic Gravity Waves Observed in the Mesosphere over the Auckland Islands during the Deep Propagating Gravity Wave Experiment (DEEPWAVE). *J. Atmos. Sci.,* **73**, 3855–3876, doi: 10.1175/JAS-D-16-0059.1.

Vosper, S. B. (2004), Inversion effects on mountain lee waves. *Q.J.R. Meteorol. Soc.,* **130**: 1723–1748. doi:10.1256/qj.03.63